Science Bulletin 65 (2020) 161–168

Contents lists available at ScienceDirect

Science Bulletin

journal homepage: www.elsevier.com/locate/scib

Science Bulletin
www.scibull.com

Article

C-V characteristics of piezotronic metal-insulator-semiconductor transistor

Jiayang Zheng [a,b,1], Yongli Zhou [c,1], Yaming Zhang [a,1], Lijie Li [d,*], Yan Zhang [a,c,e,*]

[a] School of Physics, University of Electronic Science and Technology of China, Chengdu 610054, China
[b] Department of Computer Science, University of Rochester, Rochester, NY 14627, USA
[c] Beijing Institute of Nanoenergy and Nanosystems, Chinese Academy of Sciences, Beijing 100083, China
[d] Multidisciplinary Nanotechnology Centre, College of Engineering, Swansea University, Swansea SA1 8EN, UK
[e] College of Nanoscience and Technology, University of Chinese Academy of Sciences, Beijing 100049, China

ARTICLE INFO

Article history:
Received 8 August 2019
Received in revised form 11 October 2019
Accepted 22 October 2019
Available online 5 November 2019

Keywords:
Piezotronic effect
Capacitance-voltage (C-V) characteristics
Metal-insulator-semiconductor
Distribution width of strain-induced piezoelectric charges

ABSTRACT

Third generation semiconductors for piezotronics and piezo-phototronics, such as ZnO and GaN, have both piezoelectric and semiconducting properties. Piezotronic devices normally exhibit high strain sensitivity because strain-induced piezoelectric charges control or tune the carrier transport at junctions, contacts and interfaces. The distribution width of piezoelectric charges in a junction is one of important parameters. Capacitance-voltage (C-V) characteristics can be used to estimate the distribution width of strain-induced piezoelectric charges. Piezotronic metal–insulator-semiconductor (MIS) has been modelled by analytical solutions and numerical simulations in this paper, which can serve as guidance for C-V measurements and experimental designs of piezotronic devices.

1. Introduction

Wurtzite structure semiconductors, such as ZnO and GaN exhibiting coupled piezoelectric and semiconducting properties, have been developed in many novel high performance devices [1–5]. Polarization of ions in these crystals can be used to tune or control the charge transport behavior in the nanowire based devices [6]. Piezotronics is a new emerging field for third generation semiconductor applications [1,4]. Novel nanodevices including nanogenerators [7,8], multifunctional strain-gated logic nanodevices [9], flexible transistors [10,11], high-performance piezotronic diodes [12], biomedical sensors [13] and piezophototronic LEDs [13,14] have been demonstrated with excellent performances.

Based on the fundamental theoretical framework of piezotronics [14–16], analytical solutions and numerical simulations are presented for better understanding and quantitatively calculating the carrier transport behavior in the device. Recently, models of piezotronic p-n junction, metal-semiconductor contact [15] and heterojunctions [17,18] have been studied based on the principle of piezotronic effect. Piezotronic effect on novel quantum states such as topological insulator [19], Rashba spin-orbit interaction [20] has also been studied based on quantum theory and experiments. Furthermore, piezotronic effect has been used to enhance the performance of nanodevices such as solar cells [21], the enhancement of luminescence [22–25]. Piezotronic logic units based on strain-gated transistors have been demonstrated in Refs. [26,27].

From fundamental theory of piezotronics [15], the distribution width of strain-induced piezoelectric charges is an important parameter. It is an open question to obtain the width from experiments by semiconductor physics measurement. Here, capacitance-voltage (C-V) characteristics of the metal-insulator-semiconductor (MIS) contact has been studied for providing a method to estimate the distribution width of strain-induced piezoelectric charges. We provide analytical solutions and conduct the numerical simulation using the COMSOL software package. For a typical MIS contact, a thin insulator sits between a metal contact and semiconductor, as shown in Fig. 1a. Metal serves as the gate, which controls the carrier transport by an applied gate voltage. The piezotronic MIS structure is made by a piezoelectric semiconductor material. Fig. 1b and c show a piezotronic nanowire device under tensile and compressive strain, respectively. Detailed analysis of the C-V characteristics of the device is presented in the following sections.

* Corresponding authors.
E-mail addresses: L.Li@swansea.ac.uk (L. Li), zhangyan@uestc.edu.cn (Y. Zhang).
[1] These authors contributed equally to this work.

https://doi.org/10.1016/j.scib.2019.11.001
2095-9273/

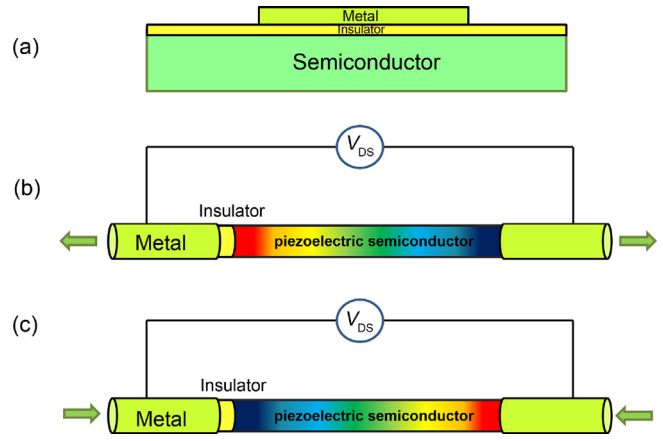

Fig. 1. (Color online) (a) Schematic of a typical metal–insulator-semiconductor (MIS) transistor. Piezotronic MIS transistor under tensile (b) and (c) compressive strain.

2. Analytical solution for 1D piezotronic MIS structure

Piezotronic theory includes electrostatic equations, current density equation and continuity equation based on semiconductor physics [28–31]. Piezoelectric equation is used to describe the induced charges under applied strain [32]. MIS structure is one of the most useful modern devices to investigate semiconductor surfaces. C-V characteristics are important for device operations [33]. A variety of theories and articles have been put forward on the MIS characteristics since the model was first presented [34–36]. An ideal and simplified model is used to study the characteristics of piezotronic MIS. For convenience, a few assumptions are made below: the working function differences between the metal and the semiconductor are neglected; surface states and other anomalies are not considered in this model; the resistance of the insulator is infinite, i.e., no current going through the insulator.

The semiconductor part of MIS is designated by a ZnO nanowire synthesized along the *c*-axis. The positive piezocharges are created at the interface of insulator and semiconductor while compressive strain is applied along the *c*-axis. As in our previous work, it is assumed that for nanodevices the piezocharges are distributed at the insulator and semiconductor interface within a width of W_{piezo}.

The ZnO is n type and the distribution of impurity is in box profile with the donor concentration N_D. Donors are fully ionized in the depletion zone; we use the Poisson's equation to calculate the electronic potential distribution in the device. The 1D model of the Poisson's equation would be degenerated to

$$-\frac{d^2\psi_i}{dx^2}=\frac{dE}{dx}=-\frac{\rho(x)}{\varepsilon_s}=\frac{1}{\varepsilon_s}[qN_D(x)+q\rho_{piezo}], \tag{1}$$

where ψ_i is electric potential, $\rho(x)$ is the charge density distribution, ε_s is the dielectric constant of the semiconductor, E is the electric field, N_D is the donor concentration, ρ_{piezo} is the piezocharges density, W_{Dn} is the depletion layer width, and d_i is the thickness of the insulator as shown in Fig. 2a. When the charge distribution is given, the electric field can be integrated using the Poisson's equation (Fig. 2b).

$$E(x)=\begin{cases}\frac{qN_D(x-W_{Dn})}{\varepsilon_s}+\frac{q\rho_{piezo}(x-W_{piezo})}{\varepsilon_s}, & (0\leqslant x\leqslant W_{piezo}),\\ \frac{qN_D(x-W_{Dn})}{\varepsilon_s}, & (W_{piezo}\leqslant x\leqslant W_{Dn}).\end{cases} \tag{2}$$

At the interface $x=0$, we can obtain the electric field in the semiconductor and insulator, respectively. According to the Poisson's equation, relationship of the two electric fields is as follows

$$E_s(0)\varepsilon_s=E_i(0)\varepsilon_i=-Q_s, \tag{3}$$

where ε_s and ε_i are the dielectric constants of the semiconductor and the insulator respectively, Q_s is the total charge in the semiconductor.

$$Q_s=q(N_DW_{Dn}+\rho_{piezo}W_{piezo}). \tag{4}$$

The potential distribution is shown in Fig. 2b. ψ_s is the surface potential of the semiconductor,

$$\psi(x)=\begin{cases}-\frac{qN_D(x-W_{Dn})^2}{2\varepsilon_s}-\frac{q\rho_{piezo}(x-W_{piezo})^2}{2\varepsilon_s}, & (0\leqslant x\leqslant W_{piezo}),\\ -\frac{qN_D(x-W_{Dn})^2}{2\varepsilon_s}, & (W_{piezo}\leqslant x\leqslant W_{Dn}).\end{cases} \tag{5}$$

The surface potential can be calculated as

$$\psi_s=\psi(0)=-\frac{q}{2\varepsilon_s}\left(N_DW_{Dn}^2+\rho_{piezo}W_{piezo}^2\right). \tag{6}$$

To calculate the total capacitance, the relation between Q_s and ψ_s should be calculated first. The external voltage is applied on both the insulator and semiconductor. As there is no charge in the insulator, the electric field is constant in the insulator.

$$V_a=V_i+\psi_s=E_id_i+\psi_s. \tag{7}$$

From Eqs. (6) and (7), we can get a quadratic equation of the depletion layer width W_{Dn}.

$$\frac{qN_D}{2\varepsilon_s}W_{Dn}^2+\frac{qN_Dd_i}{\varepsilon_i}W_{Dn}+V_a+\frac{q\rho_{piezo}W_{piezo}d_i}{\varepsilon_i}+\frac{q\rho_{piezo}W_{piezo}^2}{2\varepsilon_s}=0. \tag{8}$$

Solving Eq. (8) we can get the depletion layer width

$$W_{Dn}=-\frac{\varepsilon_sd_i}{\varepsilon_i}+\varepsilon_s\times\sqrt{\left(\frac{d_i}{\varepsilon_i}\right)^2-\frac{2}{\varepsilon_s}\left(\frac{V}{qN_D}+\frac{\rho_{piezo}W_{piezo}d_i}{\varepsilon_iN_D}+\frac{\rho_{piezo}W_{piezo}^2}{2\varepsilon_sN_D}\right)}. \tag{9}$$

The capacitance of MIS is equivalent to the total capacitance of the two capacitances of the insulator and semiconductor connected in series. The insulator is a planar plate capacitor, which is a constant. In the depletion region, the capacitance is closely related to the depletion layer width. Classical theory gives the expression of the capacitance

$$C=\frac{1}{\frac{1}{C_s}+\frac{1}{C_i}}, \tag{10}$$

where C_s is the semiconductor capacitance, C_i is the insulator capacitance and C is the total capacitance of the MIS.

The capacitances of insulator and semiconductor can be obtained by [37]

$$C_i=\frac{\varepsilon_i}{d_i}\quad C_s=\frac{\varepsilon_s}{W_{Dn}}. \tag{11}$$

Additionally, when the strain is applied at the piezoelectric semiconductor, the piezoelectric charge is [15]

$$P_z=e_{33}s_{33}=q\rho_{piezo}W_{piezo}, \tag{12}$$

where the e_{33} and s_{33} are the piezoelectric constant of material and the applied strain, respectively. The P_z is the strain induced piezoelectric polarization.

By substituting Eqs. (9), (11) and (12) to Eq. (10), the Eq. (10) is rewritten by

$$\frac{1}{C^2}=\left(\frac{d_i}{\varepsilon_i}\right)^2-\frac{2}{\varepsilon_s}\left(\frac{V}{qN_D}+\frac{e_{33}s_{33}d_i}{q\varepsilon_iN_D}+\frac{e_{33}s_{33}W_{piezo}}{2q\varepsilon_sN_D}\right). \tag{13}$$

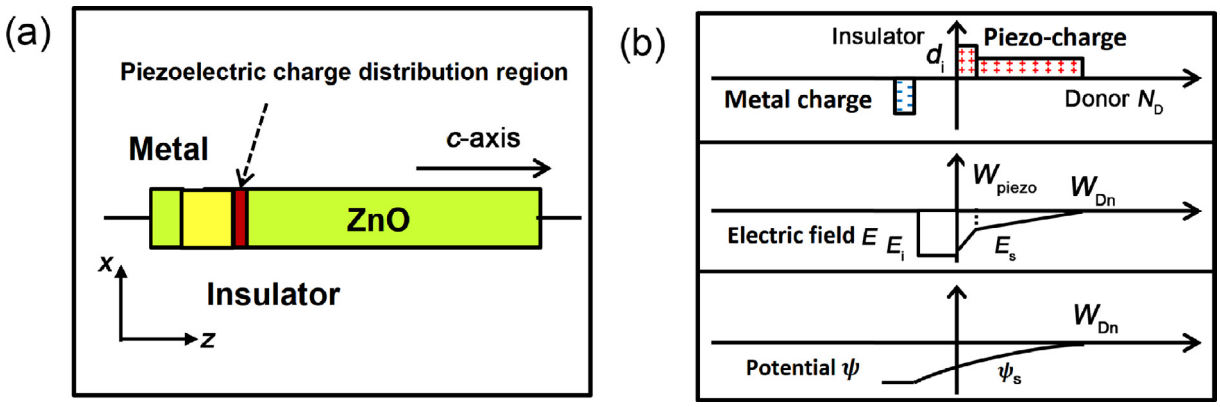

Fig. 2. (Color online) (a) Schematic of a piezotronic ZnO nanowire MIS. (b) Piezoelectric charges and donor charges distribution, electric field distribution, and potential distribution.

Moreover, the difference of $\frac{1}{C^2}$ with and without strain ($\Delta\frac{1}{C^2}$) can be given by

$$\Delta\frac{1}{C^2} = -\frac{e_{33}s_{33}}{q\varepsilon_s N_D}\left(\frac{2d_i}{\varepsilon_i}+\frac{W_{piezo}}{\varepsilon_s}\right). \quad (14)$$

Solving Eqs. (13) and (14), we can obtain the piezoelectric charges distribution width

$$W_{piezo} = -\left(\frac{q\varepsilon_s^2 N_D}{e_{33}}\frac{d1/C^2}{ds_{33}}+\frac{2\varepsilon_s d_i}{\varepsilon_i}\right). \quad (15)$$

Therefore, we can use the capacitance to estimate the piezoelectric charges distribution width. Previous works [37] have described that estimating semiconductor natural parameter by measuring C-V characteristic is a general method. In Ref. [38], it was also shown an experimental setup to measure electronic properties of piezotronic devices in different strains. By combining the traditional experimental method and piezotronic theory, we propose a MIS model to estimate piezoelectric charges distribution width. In this device structure, we only need to measure the total capacitance of MIS structure by the traditional experimental method in different strains. Finally, we can calculate and estimate the piezoelectric charges distribution width by the curves ($\Delta\frac{1}{C^2}$–s_{33}). Piezotronic and piezo-phototronic devices have promising potential applications in next-generation flexible electronics, self-powered and wearable systems [39]. In these devices, strain-induced piezoelectric charges at a contact, junction, or interface can effectively modulate and control the carrier recombination, generation, and transport properties [15,40]. Therefore, the estimation method of piezoelectric charges distribution width can be further applied for piezotronic and piezo-phototronic devices due to the analogical modulation mechanism.

For a simple case, C_s and C_i are constants, for example, $C_i = \varepsilon_i/d_i$ and $C_s = \varepsilon_s/W_{Dn}$, the total capacitance changes with the semiconductor capacitance. To qualitatively analyze the device, the negative piezocharges are generated at the interface for a tensile strain. C_s decreases while W_{Dn} increases. Obviously, the MIS capacitance C will become smaller. For the compressive strain, C becomes larger. Capacitance is influenced not only by the sign of the strain but also by the magnitude of the strain. This is the operation mechanism of the piezotronic MIS structure.

3. Numerical simulation of piezotronic MIS

The analytical solutions of piezotronic MIS give a qualitative understanding of the C-V characteristics. Here we numerically solve the equations and present a model for a better understanding of the working mechanism of the piezotronic MIS structure. The model consists of a *c*-axis n type ZnO nanowire attached to an insulator. According to fundamental theory of piezotronics, the electrical contact between the nanowire and the metal is set to be ideal Ohmic contact, so the boundary condition of electric potential and carrier concentration is Dirichlet condition. To be practical, the doping profile is described as Gaussian distribution. The general recombination process using traps in the forbidden band gap of the semiconductor is called Shockley-Read-Hall recombination.

In the simulation, the ZnO nanowire is n type, the length and radius are 80 and 10 nm. The background doping concentration is $N_{Dn} = 1\times10^{15}\,cm^{-3}$, the maximum donor doping concentration is $N_{Dn,max} = 1\times10^{17}\,cm^{-3}$. The piezoelectric constant is $e_{33} = 1.22\,C/m^2$. The intrinsic carrier density is $n_i = 1\times10^6\,cm^{-3}$, the electrons and holes mobility is $\mu_n = \mu_p = 180\,cm^2/(V\,s)$, the carrier lifetime is $\tau_n = \tau_p = 0.1\,\mu s$. The relative dielectric constants of semiconductor are $k_\perp^r = 7.77$ and $k_\parallel^r = 8.91$. The relative dielectric constants of insulator is $k_i^r = 4$. The thickness of insulator d_i = 2 nm. The control constant ch = 4.66 nm, temperature T = 300 K. The nanowire is along the *c*-axis, and the piezocharges distribution is supposed to be box profile at each end of the nanowire. The width of piezocharges is W_{piezo} = 0.25 nm in the model. The voltage is applied to the metal, and semiconductor is grounded.

Fig. 3a illustrates current-voltage characteristics of piezotronic devices. The positive strain (tensile strain) inducing negative piezoelectric charges can raise the barrier height of interface and the current subsequently decreases. By contrast, the positive piezoelectric charges at interface lowers the barrier height of interface, therefore current increases. As shown in Fig. 3b, the relative current density is a function of strain at a fixed voltage. For the strain range from −0.1% to 1%, the current varies slowly in the region of positive strains (tensile strains), however increases rapidly in the region of negative strains (compressive strains). Fig. 3c shows the capacitance C as a function of applied voltage. When the strain varies from −0.08% to 0.08%, the results suit perfectly with the analytical solution we presented. In the model, for the tensile strain, the negative piezoelectric charges are generated at the semiconductor surface, capacitance becomes smaller. For the compressive strain, the positive piezoelectric charges are generated at the semiconductor surface, capacitance becomes larger. Moreover, Fig. 3d demonstrates the theoretical Gauge Factor varies slowly at positive strain values and changes abruptly at larger negative strains in the region from −4% to 1%. This shows that the sensitivity of the piezotronic devices can reach over 10^3 in an accessibly experimental strain range.

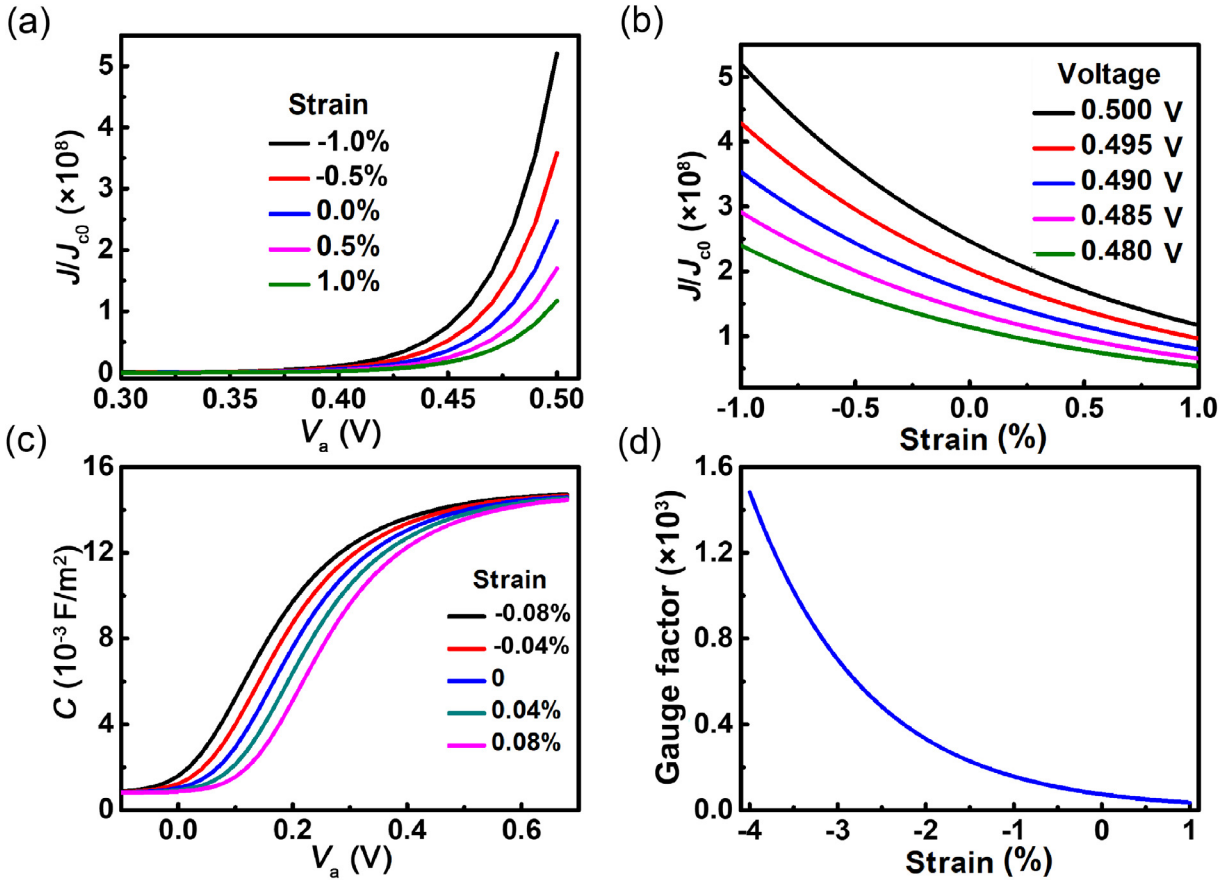

Fig. 3. (Color online) The electric characteristics of an ideal piezotronic device with piezoelectric charges. (a) The current-voltage curves at different strains from −1% to 1%. (b) Relative current density as a function of strain at different fixed voltages from 0.48 to 0.5 V. (c) Calculated capacitance *C* as a function of applied voltage at different strains from −0.08% to 0.08%. (d) Gauge Factor as a function of strain from −4% to 1%.

Fig. 4a, b shows the charge density *Q* and capacitance *C* as a function of applied strain. Fig. 5a shows the charge density *Q* as a function of surface potential ψ_s at different strains. For negative ψ_s the charge density grows very fast as the surface potential increases, which is corresponding to the accumulation region. Based on these curves we calculate the *C*-*V* curves, Fig. 5b shows the charge density *Q* as a function of applied voltage. The strain varies from −0.08% to 0.08% the result suits perfectly with the analytical solution we presented. In the model, for the tensile strain, the negative piezoelectric charges are generated at the semiconductor surface, capacitance becomes smaller. Fig. 5c and d show electrons and holes concentration in the ZnO nanowire at a fixed voltage. In the case of negative strain (or compressive strain), positive charges are accumulated at the surface which will attract electrons and repel holes. Once a positive strain (or tensile) is applied, the result will be opposite. At thermal equilibrium the carrier concentration is an exponential function of surface potential, so the charge density changes more intensively with the voltage as the electron concentration is higher.

In addition, we give the results of *C*-*V* curves and carrier concentration distribution at different doping concentrations. The background doping concentration N_{Dn} is set to 1×10^{15} cm^{-3}. The

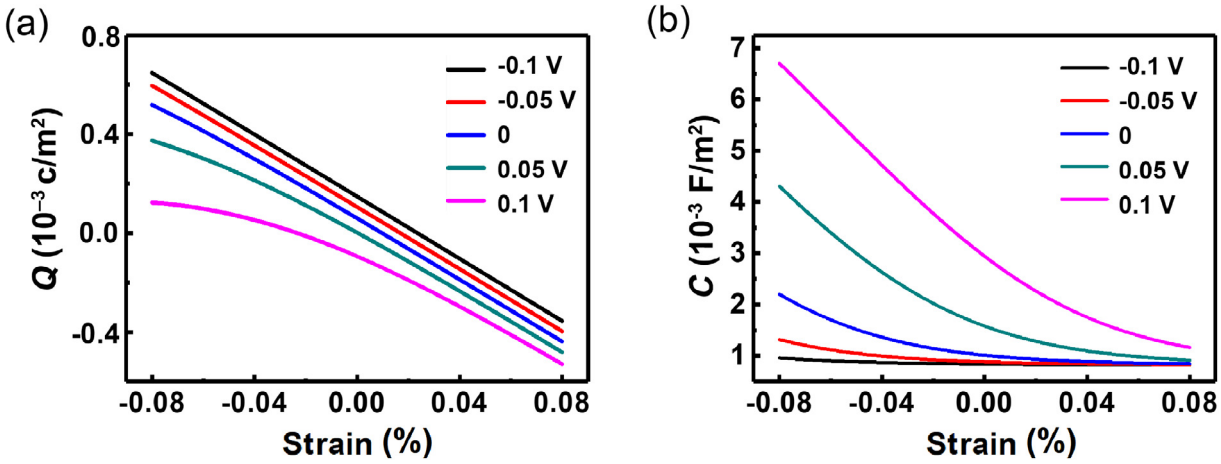

Fig. 4. (Color online) Charge (a) and capacitance (b) with different voltages across the MIS as the applied strain varies from −0.08% to 0.08%.

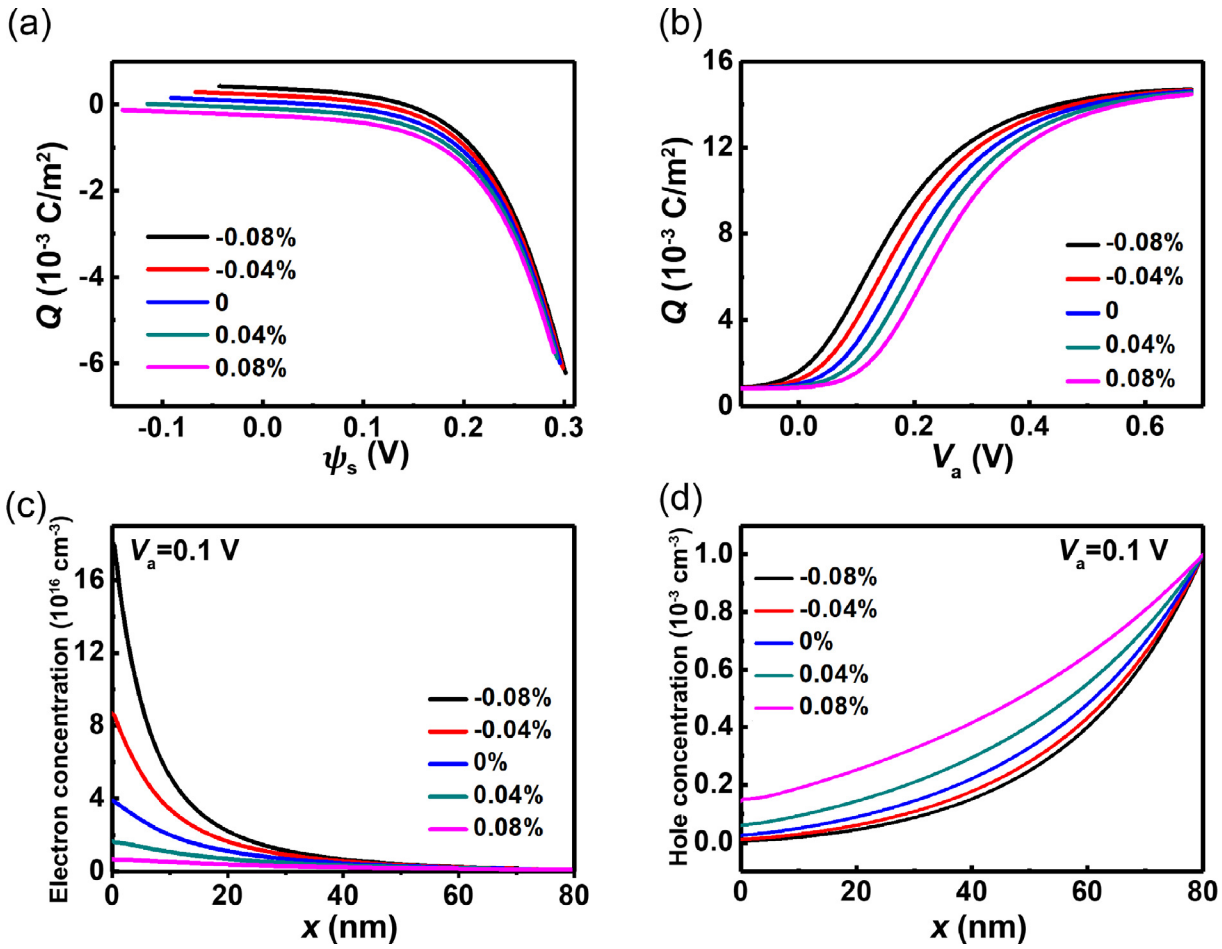

Fig. 5. (Color online) The electric characteristic of piezotronic MIS structure under different strains. (a) Calculated surface potential ψ_s and charge Q. (b) Calculated charge Q and voltage V_a. Distribution of electrons (c) and distribution of holes (d) at a fixed voltage of 0.1 V across the MIS for the applied strain varying from −0.08% to 0.08%.

maximum donor concentration varies from 5×10^{16} to 1×10^{18} cm^{-3}, as shown in Fig. 6. As it can be seen from Eq. (12), W_{Dn} get thinner as N_D varies from 5×10^{16} to 1×10^{18} cm^{-3}, thus the capacitance becomes larger. The curves shown in Fig. 6b illustrate that donor concentration has a major influence on the C-V characteristics. The electrons and holes concentration distributions are also given in Fig. 6c and d.

Fig. 7a demonstrates $\Delta\frac{1}{C^2}$ as a function of applied strain at different piezoelectric charge distribution widths. The $|\Delta\frac{1}{C^2}|$ increases with the raising strain. This shows that the strains have obvious influence on the total capacitance. In addition, the $|\Delta\frac{1}{C^2}|$ has more obvious varieties in a greater W_{piezo} at the same strain from the enlargement part. Fig. 7b and c show $\Delta\frac{1}{C^2}$ as a function of W_{piezo} at tensile and compressive strains, respectively. The result is consistent with Fig. 7a. Fig. 7d illustrates $\frac{d1/C^2}{ds_{33}}$ as a function of strain and it is a constant. Moreover, the $\frac{d1/C^2}{ds_{33}}$ has different values in different W_{piezo}. Therefore, we can calculate piezoelectric charges distribution width by measuring total capacitance of devices. Previous works [15] show performance and the physical control mechanism of piezotronic devices. Meanwhile, the authors firstly proposed W_{piezo} and investigated the importance of W_{piezo} on performance of piezotronic devices. However, how to estimate W_{piezo} is still a challenging task. In this study, we propose a method by analyzing C-V characteristic of MIS structure and combining the traditional measurement method and piezotronic theory to estimate W_{piezo}. Meanwhile, the method is general and mature in estimating semiconductor intrinsic parameters [37]. Thus, analyzing C-V characteristic of MIS structure to estimate the value of W_{piezo} is a feasible approach in the experiment.

Optoelectronic devices consisting of metal-insulator-ZnO nanowire have been investigated in several previous papers [41,42]. In addition, ZnO thin film-based MIS structure have also been fully investigated for electronic devices [43–45]. Besides, the thin insulator layer usually exists between metal and semiconductor in one end and the other end is only comprised of metal and semiconductor. Importantly, recent research [46] has demonstrated ZnO thin film grown along *c*-axial in the experiment. Therefore, the devices can also be built by metal-insulator-ZnO thin film along *c*-axial. Like above researches, we adopt a typical MIS structure consisting of metal-insulator-piezoelectric semiconductor as analytic model in our study. Hence, we can use it to calculate the piezoelectric charges distribution width.

Moreover, in order to efficiently examine semiconductor intrinsic properties of the MIS structure, we adopt a novel approach based on neural network models. For simplicity, we train and test our neural network model based on the *Q*-*V* curves in Fig. 5b. We treat these curves as linear functions and find the correlation between the linear part and the strain value. The intercept of each linear part is calculated and then used as input value to our neural network while strain value is used as the target value to train it. The process to obtain our neural network model is demonstrated in Fig. 8a. Our neural network is a simple doubly layered feed-forward neural network using identity activation linear function with one input unit, one hidden layer consisting of three hidden

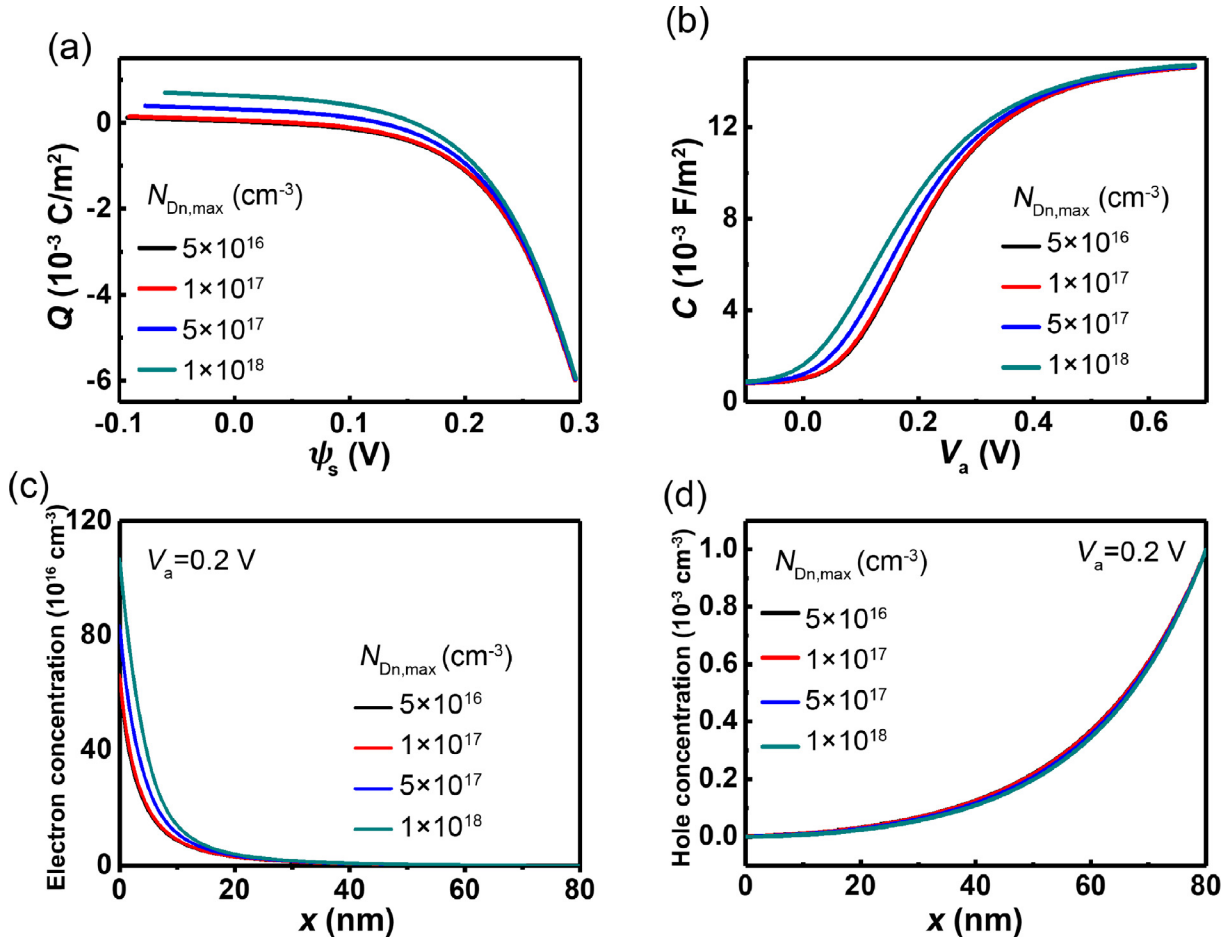

Fig. 6. (Color online) The electric characteristic of piezotronic MIS structure at different doping concentrations. (a) Calculated piezotronic MIS $Q-\psi_s$ curves and (b) *C-V* curves at different maximum donor doping concentrations (c) holes and (d) electrons distribution at an applied forward voltage of 0.2 V at different maximum donor doping concentrations.

units, and one output unit to accommodate the continuous property of the strain value [51]. We train our neural network using back-propagation with mean squared error as loss function [47]. A validation dataset, consisting of 100 data points, is generated through the calculated linear relation between intercept and strain value. We use this validation dataset as inputs to the trained neural network to produce corresponding predictions and test the accuracy and validity of our model. As shown in Fig. 8b, our model starts to exhibit 100% prediction accuracy at around iteration 50 with learning rate of 0.01 on our validation dataset. With this result, we are confident to say that neural network has promising potential application for examining intrinsic characteristics of semiconductors with sufficient efficiency and accuracy.

Among conventional methods of analyzing the simulation results, the most commonly used ones are still based on curve fitting to approximate the result [48]. These methods, such as the least-squares method, usually utilize implicit functions (including both independent and dependent variables) to express their target variables [48]. Because of the existence of both independent and dependent variables, complexity of analyzing the simulation result increases and errors can also be introduced [48]. Additionally, nonlinear fitting algorithms, such as quasi-Newton method, have also been proposed to extract intrinsic properties of the simulation result. However, these methods do not guarantee an accurate result at convergence if the initial value is not carefully chosen [49]. On the other hand, neural networks do not need to learn with pre-defined target variable expressions and is capable of learning any functions [51]. Although learning in neural networks relies on the optimization of a non-convex function in this task, the local minimums are actually very close to the global minimum when the neural networks is fully connected (each unit in each layer connects to all units in the next layer) [47]. As a result, even an arbitrary initial value can lead to an accurate result in very few training iterations (only about 40–50 iterations). Moreover, since there are often extensive experimental data, neural networks can utilize these data and do not require using experts' knowledge by directly classifying based on simulation result [50].

4. Conclusion

We present a numerical model of a piezotronic MIS for analyzing the effect of the piezocharges on its C-V characteristics. Analytical solutions are given in this work to introduce the mechanism of the piezotronic MIS. Numerical simulation is also presented to demonstrate a better understanding of the model. We find that the total capacitance becomes smaller when negative piezocharges generated at the interface and becomes larger when positive piezocharges are generated. This work can be utilized as guidance for future device design and implementation.

Conflict of interest

The authors declare that they have no conflict of interest.

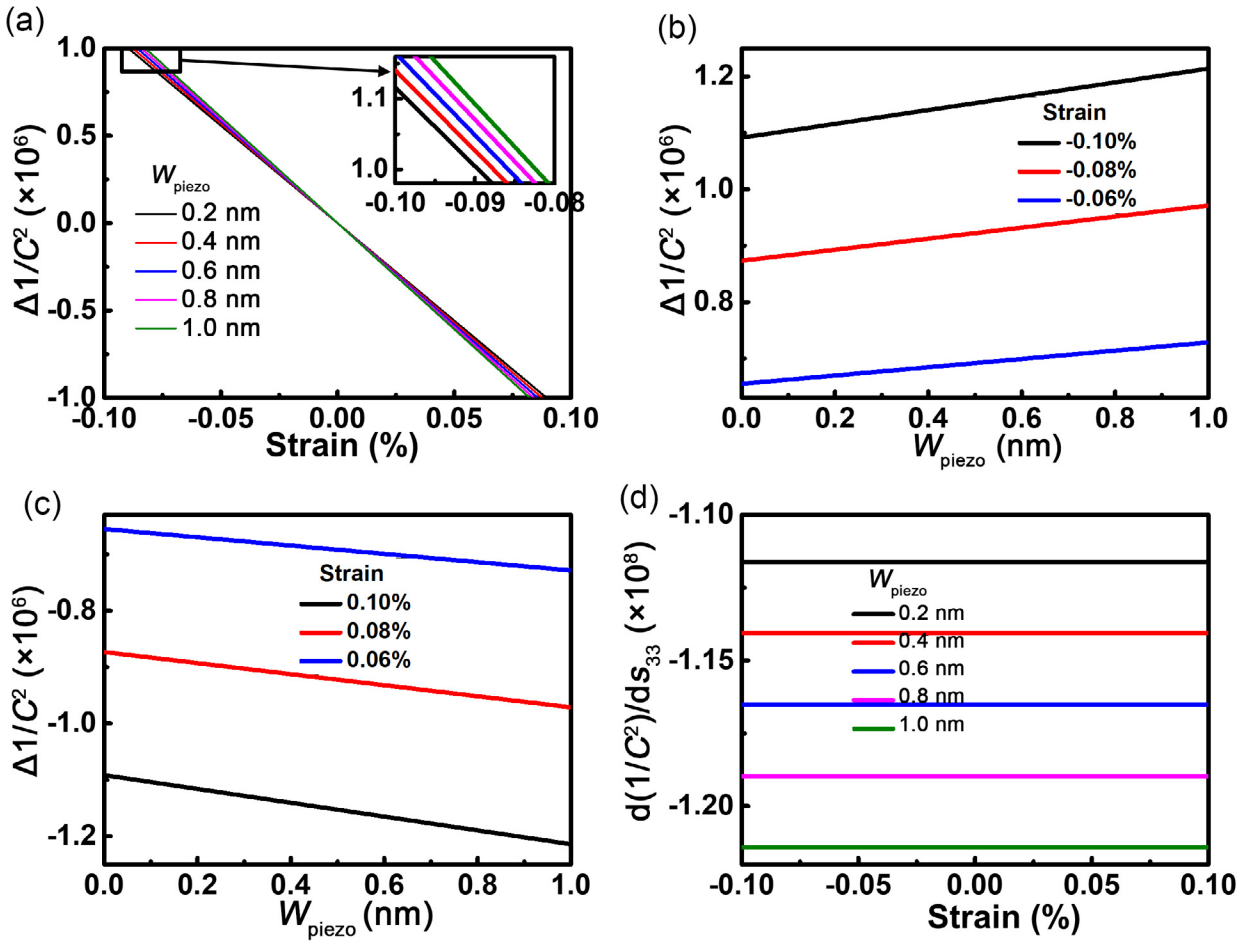

Fig. 7. (Color online) Relation of capacitance and piezoelectric charges distribution width. (a) Calculated $\Delta\frac{1}{C^2}$ as a function of strain at different piezoelectric charges distribution width. (b, c) $\Delta\frac{1}{C^2}$ as a relation of piezoelectric charges distribution width at tensile and compressive strain, respectively. (d) $\mathrm{d}\frac{1}{C^2}/\mathrm{ds}_{33}$ as a function of strain at different piezoelectric charges distribution width.

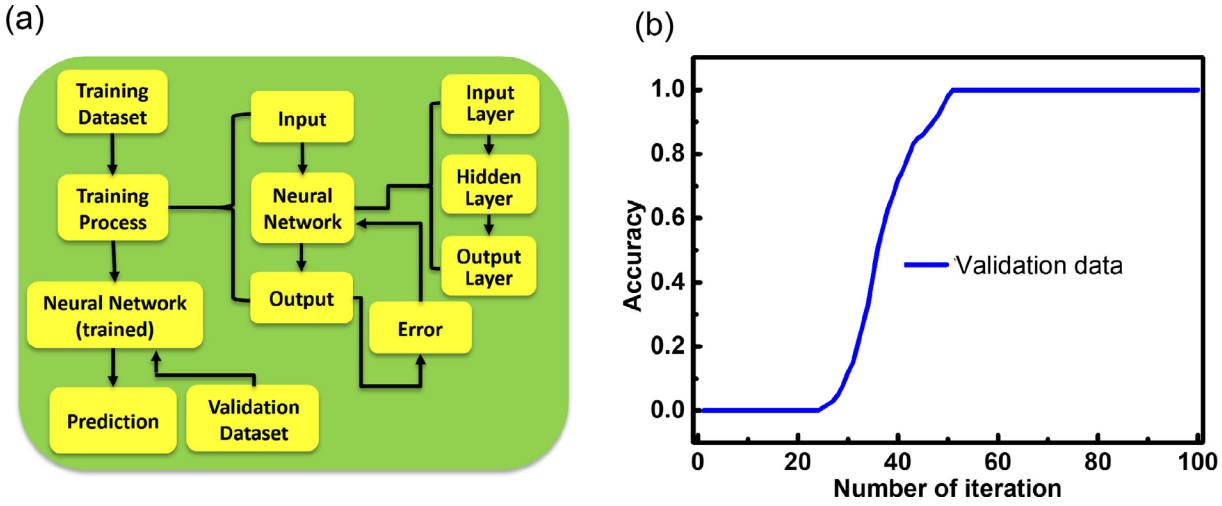

Fig. 8. (Color online) (a) Procedure of our experiment consists of training process and inference process after obtaining trained neural network. (b) Accuracy on validation set as a function of number of training process iteration. The presented result is achieved using 100 iterations and 0.01 learning rate.

Acknowledgments

The authors are thankful for the support from Swansea University, Solar Photovoltaic Academic Research Consortium (SPARC) II project, and University of Electronic Science and Technology of China.

Author contributions

Jiayang Zheng, Yongli Zhou, and Yaming Zhang contributed equally to this work. Yan Zhang conceived the idea and guided this work. Jiayang Zheng, Yongli Zhou, Yaming Zhang, and Yan Zhang fabricated theoretic frame and analysed the data. Jiayang Zheng, Yongli

Zhou, Yaming Zhang, Lijie Li, and Yan Zhang wrote this paper. All the authors discussed the results and commented on the manuscript.

References

[1] Wu WZ, Wang ZL. Piezotronics and piezo-phototronics for adaptive electronics and optoelectronics. Nat Rev Mater 2016;1:UNSP 16031.
[2] Du C, Hu W, Wang ZL. Recent progress on piezotronic and piezo-phototronic effects in III-group nitride devices and applications. Adv Eng Mater 2017;20:1700760.
[3] Zhao ZF, Pu X, Han CB, et al. Piezotronic effect in polarity-controlled GaN nanowires. ACS Nano 2015;9:8578–83.
[4] Jenkins K, Nguyen V, Zhu R, et al. Piezotronic effect: an emerging mechanism for sensing applications. Sensors 2015;15:22914–40.
[5] Zhu R, Yang R. Synthesis and characterization of piezotronic materials for application in strain/stress sensing. Berlin: Springer; 2018. p. 1–4.
[6] Liu Y, Zhang Y, Yang Q, et al. Fundamental theories of piezotronics and piezo-phototronics. Nano Energy 2015;14:257–75.
[7] Wang ZL, Song J. Piezoelectric nanogenerators based on zinc oxide nanowire arrays. Science 2006;312:242–6.
[8] Qin Y, Wang X, Wang ZL. Microfibre-nanowire hybrid structure for energy scavenging. Nature 2008;451:809–13.
[9] Yu R, Wu W, Pan C, et al. Piezo-phototronic Boolean logic and computation using photon and strain dual-gated nanowire transistors. Adv Mater 2015;27:940–7.
[10] Han W, Zhou Y, Zhang Y, et al. Strain-gated piezotronic transistors based on vertical zinc oxide nanowires. ACS Nano 2012;6:3760–6.
[11] Wu W, Wen X, Wang ZL. Taxel-addressable matrix of vertical-nanowire piezotronic transistors for active and adaptive tactile imaging. Science 2013;340:952–7.
[12] He JH, Hsin CL, Liu J, et al. Piezoelectric gated diode of a single ZnO nanowire. Adv Mater 2007;19:781–4.
[13] Cao X, Cao X, Guo H, et al. Piezotronic effect enhanced label-free detection of DNA using a schottky-contacted ZnO nanowire biosensor. ACS Nano 2016;10:8038–44.
[14] Zhang Y, Wang ZL. Theory of piezo-phototronics for light-emitting diodes. Adv Mater 2012;24:4712–8.
[15] Zhang Y, Liu Y, Wang ZL. Fundamental theory of piezotronics. Adv Mater 2011;23:3004–13.
[16] Zhang Y, Yang Y, Wang ZL. Piezo-phototronics effect on nano/microwire solar cells. Energy Environ Sci 2012;5:6850.
[17] Shi J, Starr MB, Wang X. Band structure engineering at heterojunction interfaces via the piezotronic effect. Adv Mater 2012;24:4683–91.
[18] Wang X, Yu R, Jiang C, et al. Piezotronic effect modulated heterojunction electron gas in AlGaN/AlN/GaN heterostructure microwire. Adv Mater 2016;28:7234–42.
[19] Hu G, Zhang Y, Li L, et al. Piezotronic transistor based on topological insulators. ACS Nano 2018;12:779–85.
[20] Zhu L, Zhang Y, Lin P, et al. Piezotronic effect on rashba spin-orbit coupling in a ZnO/P3HT nanowire array structure. ACS Nano 2018;12:1811–20.
[21] Zheng DQ, Zhao ZM, Huang R, et al. High-performance piezo-phototronic solar cell based on two-dimensional materials. Nano Energy 2017;32:448–53.
[22] Zhang Y, Li LJ. Piezophototronic effect enhanced luminescence of zinc oxide nanowires. Nano Energy 2016;22:533–8.
[23] Li LJ, Zhang Y. Simulation of wavelength selection using ZnO nanowires array. J Appl Phys 2017;121:214302.
[24] Li LJ, Zhang Y. Controlling the luminescence of monolayer MoS_2 based on the piezoelectric effect. Nano Res 2017;10:2527–34.
[25] Zhang Y, Nie J, Li L. Piezotronic effect on the luminescence of quantum dots for micro/nano-newton force measurement. Nano Res 2018;11:1977–86.
[26] Wu W, Wei Y, Wang ZL. Strain-gated piezotronic logic nanodevices. Adv Mater 2010;22:4711–5.
[27] Nie J, Hu G, Li L, et al. Piezotronic analog-to-digital converters based on strain-gated transistors. Nano Energy 2018;46:423–7.
[28] Sze SM. Physics of semiconductor devices. New York: Wiley; 1981.
[29] Bethe HA, Laboratory MIoTR. Theory of the Boundary Layer of Crystal Rectifiers. Radiation Laboratory, Massachusetts Institute of Technology; 1942.
[30] Crowell CR, Sze SM. Current transport in metal-semiconductor barriers. Solid State Electron 1966;9:1035–48.
[31] Schottky W. Halbleitertheorie der Sperrschicht. Naturwissenschaften 1938;26:843.
[32] Ikeda T. Fundamentals of piezoelectricity. Oxford: Oxford University Press; 1996.
[33] Terman LM. An investigation of surface states at a silicon/silicon oxide interface employing metal-oxide-silicon diodes. Solid State Electron 1962;5:285–99.
[34] Lindner R. Semiconductor surface varactor. Bell System Technol J 1962;41:803–31.
[35] Grove AS, Snow EH, Deal BE, et al. Simple physical model for the space-charge capacitance of metal-oxide-semiconductor structures. J Appl Phys 1964;35:2458.
[36] Frankl DR. Some effects of material parameters on the design of surface space-charge varactors. Solid State Electron 1961;2:71–6.
[37] Sze SM, Ng KK. Physics of Semiconductor Devices. New Jersey: Wiley; 2007.
[38] Hu Y, Zhang Y, Lin L, et al. Piezo-phototronic effect on electroluminescence properties of p-type GaN thin films. Nano Lett 2012;12:3851–6.
[39] Pan C, Zhai J, Wang ZL. Piezotronics and Piezo-phototronics of third generation semiconductor nanowires. Chem Rev 2019;119:9303–59.
[40] Zhang Y, Leng Y, Willatzen M, et al. Theory of piezotronics and piezo-phototronics. MRS Bull 2018;43:928–35.
[41] Liao Q, Liang M, Zhang Z, et al. Strain-modulation and service behavior of Au-MgO-ZnO ultraviolet photodetector by piezo-phototronic effect. Nano Res 2015;8:3772–9.
[42] Liu Y, Xu H, Liu C, et al. Recent progress in ZnO-based heterojunction ultraviolet light-emitting devices. Chin Sci Bull 2014;59:1219–27.
[43] Alivov YI, Look DC, Ataev BM, et al. Fabrication of ZnO-based metal–insulator–semiconductor diodes by ion implantation. Solid State Electron 2004;48:2343–6.
[44] Young SJ, Ji LW, Chang SJ, et al. ZnO-based MIS photodetectors. Sens Actuators A Phys 2008;141:225–9.
[45] Liu CY, Xu HY, Sun Y, et al. ZnO ultraviolet random laser diode on metal copper substrate. Opt Express 2014;22:16731–7.
[46] Wang L, Liu S, Zhang Z, et al. 2D piezotronics in atomically thin zinc oxide sheets: interfacing gating and channel width gating. Nano Energy 2019;60:724–33.
[47] Rumelhart DE, Hinton GE, Williams RJ. Learning representations by back-propagating errors. Nature 1986;323:533–6.
[48] Zhang C, Zhang J, Hao Y, et al. A simple and efficient solar cell parameter extraction method from a single current-voltage curve. J Appl Phys 2011;110:064504.
[49] Ye M, Wang X, Xu Y. Parameter extraction of solar cells using particle swarm optimization. J Appl Phys 2009;105:094502.
[50] Irani KB, Cheng J, Fayyad UM, et al. Applying machine learning to semiconductor manufacturing. IEEE Expert 1993;8:41–7.
[51] Bishop CM. Pattern recorgnition and machine learning. Berlin: Springer; 2006.

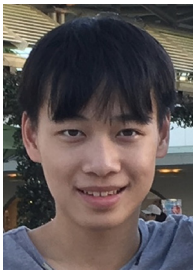

Jiayang Zhang currently is an undergraduate at University of Rochester. He is working on his B.S. degree in the Department of Computer Science and B.A. degree in the Department of Mathematics. He was working remotely in Prof. Yan Zhang's group. He is interested in machine learning and computer vision, especially developing new intelligent systems that can be used to facilitate scientific development.

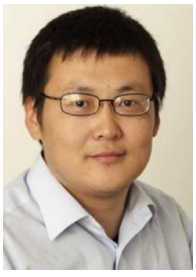

Lijie Li is a professor at Swansea University, UK. His research interests are design, modeling, fabrication, and characterization of MEMS, NEMS, sensors and actuators.

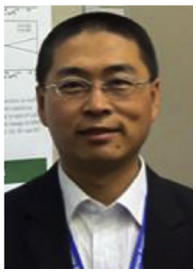

Yan Zhang is a professor at University of Electronic Science and Technology of China. He received his B. S. degree (1995) and Ph.D degree in Theoretical Physics (2004) from Lanzhou University. His research interests include self-powered nano/micro system, piezotronic and modeling of nonlinear dynamics of NEMS.